VOL. 11, NO. 2, JANUARY 2016 ISSN 1819-6608
ARPN Journal of Engineering and Applied Sciences

www.arpnjournals.com

FLOW AND HEAT TRANSFER ENHANCEMENT AROUND STAGGERED TUBES USING RECTANGULAR VORTEX GENERATORS

Prabowo, Melvin Emil S., Nanang R. and Rizki Anggiansyah
Department of Mechanical Engineering, ITS Surabaya, Indonesia
E-Mail: prabowo@me.its.ac.id

ABSTRACT

Numerical analysis was carried out to study the flow and heat transfer characteristics around staggered tubes with rectangular vortex generators (VGs) mounted behind the tubes. The effect of location VGs in different span angle from stagnation point ($\Phi=120^0$, 135^0 and 140^0) were investigated in detail while the Reynolds number based on diameter tube was kept constant at $Re_D=2959$. The numerical results are also analyzed from the correlation between the contour velocity and temperature gradients which is a basic mechanism of heat transfer. The results indicated that the rectangular VGs is able to improve the convection heat transfer on the rear part of upstream tube and forepart of downstream tube. The average Nu was shown to increase by 8%-78% and it is found that the location VGs on $\Phi=120^0$ provides the best heat transfer augmentation.

Keywords: heat transfer enhancement, vortex generators, staggered tubes, CFD.

INTRODUCTION

Fin and tube heat exchangers are usually used compact heat exchanger in various fields such as chemical industry, power generation, air conditioning and automobile. For typical application, the enhancement of heat transfer in fin and tube is critical to improve the overall performance of heat exchangers. The heat transfer coefficient on the air-side is typically low due to the thermophysical air property and relative low velocity. In order to increase heat transfer on the air side and leads to small penalties in pressure drop, a common method is to apply vortex generators (VGs), such as ribs, wins and winglet. When the fluids through VGs, vortices are generated due to the friction and separation on the edge the vortex generators.

In the recent year, the studies on heat transfer and flow structure with longitudinal VGs in fin and tube heat exchanger has taken more attention. Chu *et al* [1] studied the flow and heat transfer of an air stream over rectangular winglet pair (RWP) with three configurations; 1, 3 and 7 RWP for inline tubes. The air-side heat transfer coefficient improves by 28.1-131% with an associated pressure drop penalty increase 11-121% for three enhanced configurations. Gang Lie *et al* [2] was found that the delta-winglet vortex generators with attack angle and an aspect ratio produce the longitudinal vortices and accelerate the flow. The result indicates significant augmentation of heat transfer with modest pressure drop penalties. Kannan and Kumar [3] also studied the effect of different span angle vortex generators. The results indicated that the triangle shape winglet is able to generate longitudinal vortices and improve the heat transfer performance in the wake regions. Yuh Jang *et al* [4] numerically investigated optimization of the span angle and location of vortex generators in plate fin and tube heat exchanger. The result show that for both in-line and staggered arrangement, as the span angle and transverse location are increased, the strength of the longitudinal vortex is intensified and both *j-Colburn* and *f*-friction factors are increased. Wu and Tao [5] numerically studied the heat transfer on a fin and tube heat exchanger in aligned arrangement with delta winglet pairs. The mechanism can be explained by field synergy principle.

The forgoing literature reviews show that have not done comparison study of flow and heat transfer around tubes for different location vortex generators for tube banks in staggered arrangement. This has motivated the present investigation.

MODEL DESCRIPTION

Meshing was developed in Gambit software as described in Figure-2 (a) and (b). Quadrilateral-map used due to complexity geometry of domain and best mesh for converge. Meshing around tube and obstacle made more closely to get accuracy of simulation. Tube and obstacle set as stationary wall. Grid independency have been made and obtained that 108576 cells is the best compare to others i.e. 42484, 62016 and 125904 cells.

Numerical simulation is to perform by a computational fluid dynamics for fluid flow and heat transfer around tube banks using CFD. The comparisons of heat transfer around tube banks without (baseline) and with VGs under different span angle from stagnation point $\Phi=120^0$, 135^0 and 150^0 carried out with the inlet air velocity and temperature are 5 m/s and 305 K, respectively. Tube and VGs dimension have been written in Table-1, while computational domain was shown in Figure 1 (a) and (b). The entrance length of upstream was 6D to make the flow become as fully developed flow when entering the tube banks. While the length of downstream was made 12D to guarantee reverse flow not occur.

Fluid assumed to be incompressible with constant property and the flow in steady state condition. This

simulation was performing in 2D double precision due to heat transfer with high thermal conductivity and use segregated solver. K–ε RNG model was used for turbulence model in this simulation due to vortex and low Reynold number. Inlet boundary condition was assumed as uniform flow and set as velocity inlet. The airflow direction is x-direction. Outlet was set as outflow. Upper and lower boundary condition set as symmetry. Discretization of momentum and energy set to second order upwind scheme and velocity and pressure was set to coupling. All of convergence criterion was set to 10^{-3} except energy was set to 10^{-6}.

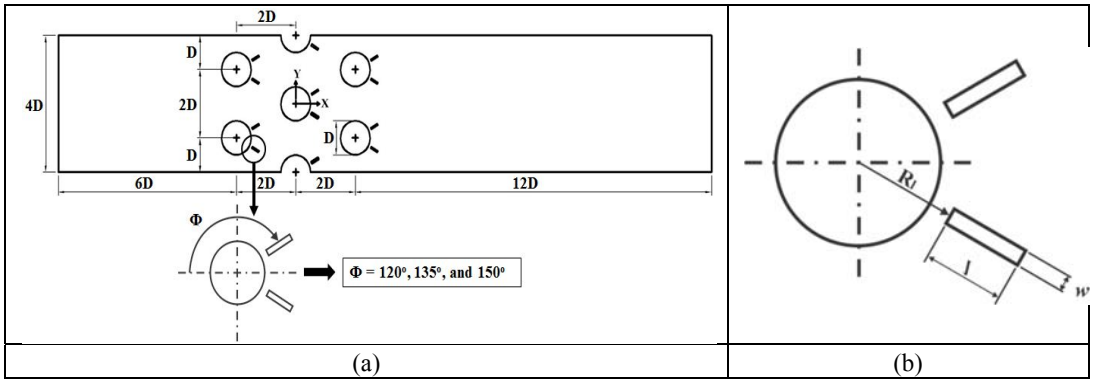

Figure-1. Computational domain: (a) Geometry of staggered tube arrangement and (b) Rectangular VGs.

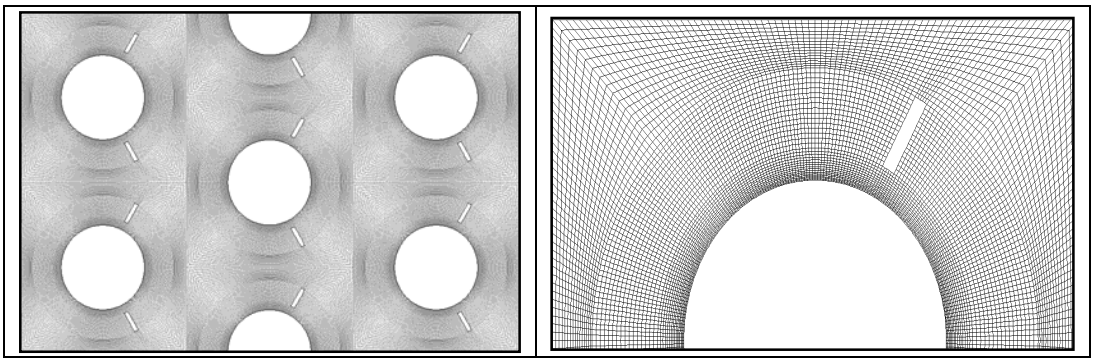

Figure-2. Meshing quadrilateral-map: (a) Tube with rectangular VGs and (b) Zoom in around tube

Table-1. Tube and VGs dimension.

Dimension	Value
Tube outside diameter (mm)	10
Tube row number	3
Tube wall temperature, K	347
Width, w (mm)	0.5
Length, *l* (mm)	2.5
Radial distance, R_l/D	0.6

RESULT AND DISCUSSIONS

Flow Pattern

Figure-3 presents the comparisons of velocity contour for baseline model (without VG) and three different location of VGs with angle from stagnation point $\Phi=120^0$, 135^0 and 140^0. For the baseline model, it can be seen that the longitudinal flow passes around the circular tubes and is accelerated in the region transverse for the first to third row of the tube. It forms wake region behind the tubes. The addition of VGs results in the flow dividing into two streams. One stream passes over the VGs and accelerates the local flow velocity at forepart of the second to third row of tubes. This leads to increased heat transfer at the forepart of tubes. The VGs for $\Phi=120^0$ induces greater accelerates longitudinal flow when compare to

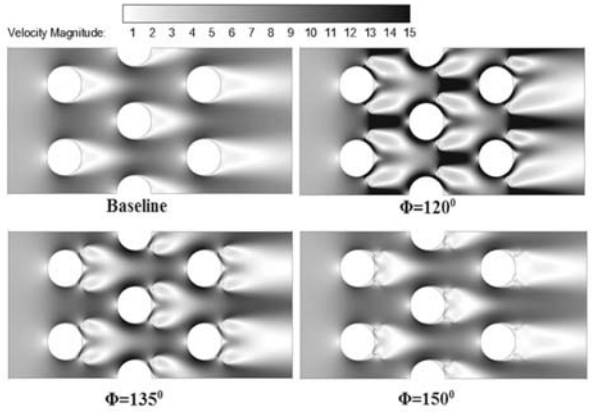

Figure-3. Velocity contour for baseline and with rectangular VGs on different angle; unit (m/s).

$\Phi=135^0$ or 140^0. Meanwhile, the other stream flows into wake region behind tube and accelerate the local flow velocity at rear part of the tube which delay the boundary layer separation from the tube. This brings to improve the heat transfer rate in the wake region.

Figure-4 illustrates comparisons of temperature gradient for the baseline and three VGs models. Air temperature gradient in the inlet region is shown same contour for all model. As the air approaches the VG, the

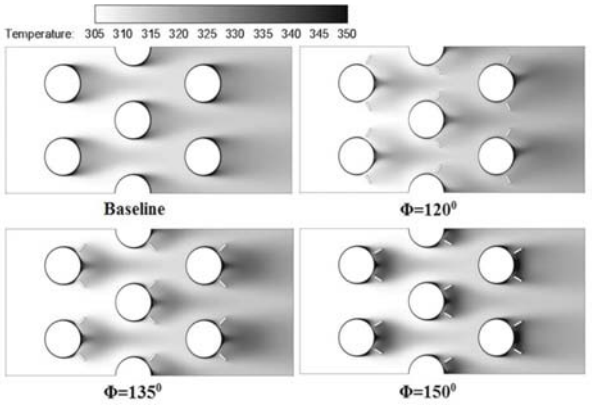

Figure-4. Temperature gradient for baseline and with rectangular VGs on different angle; unit (K).

enhancement of heat transfer notable on downstream tube row. The air temperature behind the tubes is distinctly lower when VGs is used. This means that heat transfer performance is become better at the wake region. In addition, the air temperature at front of tube for second to third row shows significantly decreased due to the flow passes on the VGs. Beside that, the air temperature at the outlet region is raised when compared with baseline model. Using VGs show that heat transfer performance improvements are found in the rear part of tube and forepart of tube in the downstream of flow.

Figure-5 represents circumferential velocity (V_θ) of the 1st row of tube for baseline and three different span angle VGs model. At the stagnation point, V_θ have value 0, then increases with the increase in θ up to a maximum at $\theta=60^0$, then decreases to $V_\theta=0$ which indicates to the separation point where $\theta=100^0$. It is observed that the distribution of V_θ is symmetrical from stagnation point until $\theta=80^0$. This explain that there is no difference in the flow of the front of the tube for four models. However, asymmetrical show $\theta>80^0$ for baseline and three different Φ of the VGs. When VGs is used, the flow is accelerated by gap between VGs and tube wall. This leads to the separation point is delayed to rear part of tube (wake region), even VGs with $\Phi=120^0$ until the angle of $\theta=150^0$.

Figure-6 shows local Nusselt number (Nu_θ) distribution of the 1st row of tube for baseline and three different span angle VGs model. The Nu_θ is the highest at stagnation point and decreases gradually along surface tube until minimum value at separation point and than increase again due to wake region. For baseline model and three different angle VGs model, the distribution of Nu_θ behave similarly up to $\theta=80^0$. For $\theta>80^0$, however, the Nu_θ distribution shows sharp increase at the gap between VGs and tube wall then continued to decline on a narrow area of the wake region. The distribution of Nu_θ have a similar distribution of V_θ as shown in the Figure-5.

Figure-7 represents the circumferential velocity (V_θ) of the 2nd row of tube for baseline and three different span angle VGs model. In the range of θ ($0 \le \theta \le 30^0$), the V_θ distribution shows significantly increased start from stagnation point. This indicates an increase in flow velocity on the front surface of the tube when the VG used.

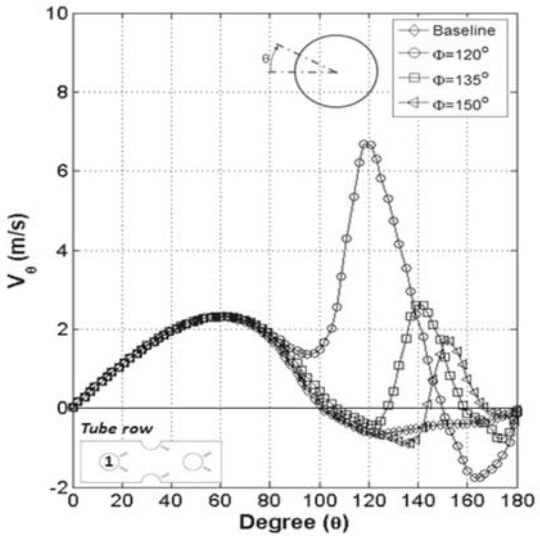

Figure-5. The circumferential velocity (V_θ) of the 1st row of tube.

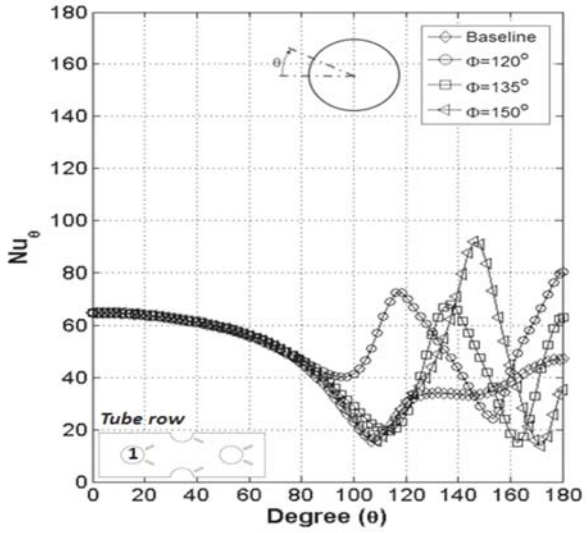

Figure-6. The Local Nusselt number (Nu_θ) distribution of the 1st row of tube.

The same distribution of V_θ also occurs on the rear surface of the tube. The effect of the VGs span angle on V_θ distribution occurred in increased flow velocity on the surface of the front and rear of tube.

Figure-8 displays the local Nusselt number (Nu_θ) distribution of the 2nd row of tube for baseline and three different span angle VGs model. As known, the value of Nu_θ is the highest at stagnation point and decreases gradually along surface tube until minimum value at separation point and then increase again due to wake region. The addition of VGs causes a significant increase

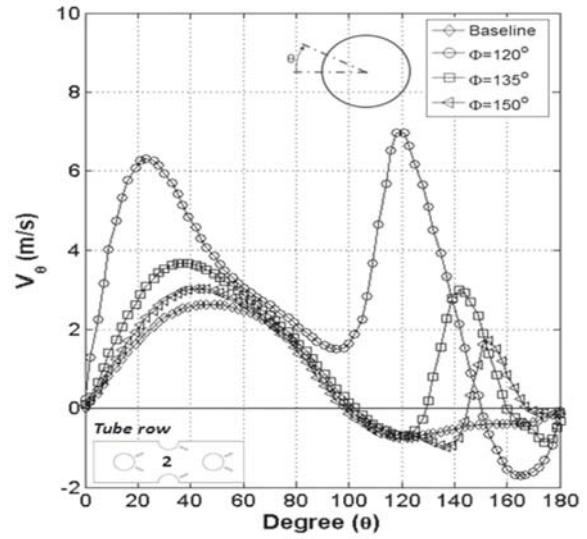

Figure-7. The represents circumferential velocity (V_θ) of the 2nd row of tube.

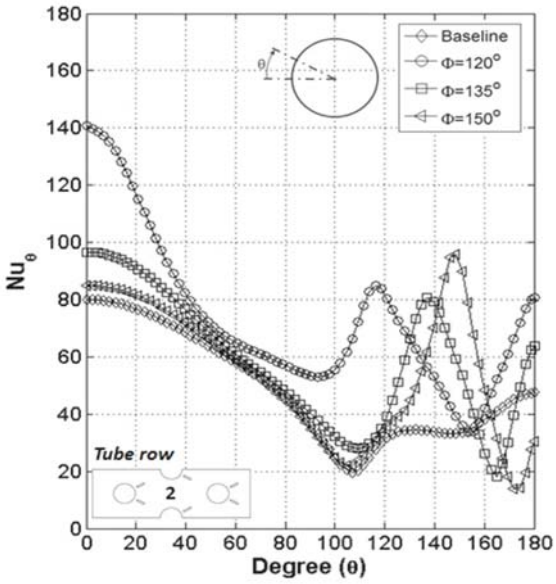

Figure-8. The local Nusselt number (Nu_θ) distribution of the 2nd row of tube.

then decreases to $V_\theta=0$ which indicates to the separation point where $\theta=100^0$. It is observed that the distribution of V_θ is symmetrical from stagnation point until $\theta=80^0$. This explain that there is no difference in the flow of the front of the tube for four models. However, asymmetrical show $\theta>80^0$ for baseline and three different Φ of the VGs. When VGs is used, the flow is accelerated by gap between VGs and wall tube. This leads to the separation point is delayed

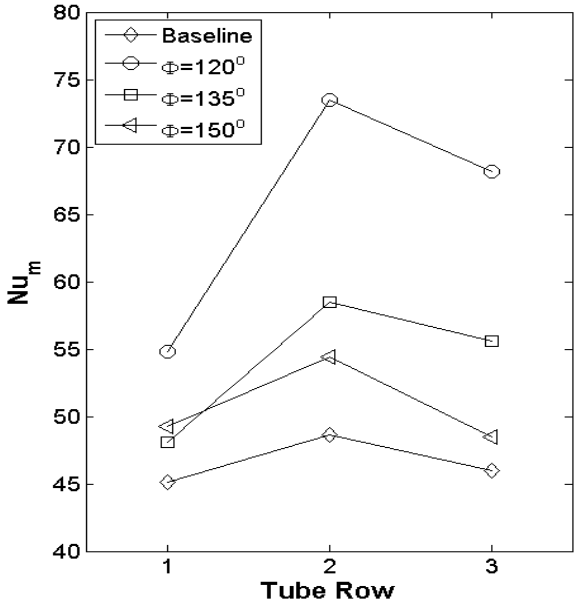

Figure-9. The average Nusselt number (Nu_m) of tubes in each row.

to rear part of tube (wake region), even VGs with $\Phi=120^0$ until the angle of $\theta=150^0$.

Figure-9 shows average Nusselt number (Nu_m) of tubes in each row for baseline and three different span angle VGs model. For the 1st row of tube, the Nu_m slightly increase of 9-21% when compared to baseline (without VGs) due to rise in local Nusselt number (Nu_θ) at rear part of tube as described in Figure-6. Meanwhile, for the 2nd row of tube, Nu_m significant increase of 32-78% which is caused by increasing Nu_θ at forepart and rear part of tube. While, for the 3rd row of tube, Nu_m has same tendency with the 2nd row of tube with an rise of 8 - 68%.

CONCLUSIONS

Flow and heat transfer over 3-row of tube in staggered arrangement without (baseline) and with VGs in three different span angle from stagnation point $\Phi=120^0$, 135^0 and 140^0 are studied numerically. The following conclusion can be drawn:

a) The addition of VGs results in the incoming flow dividing into two streams. One stream passes over the VGs and accelerates the local flow velocity at forepart of the second to third row of tubes. The other stream flows into wake region behind tube and accelerate the local flow velocity at rear part of the tube which delay the boundary layer separation from the tube.
b) The rectangular VGs is able to improve the local Nusselt number (Nu□□□) on the rear part of upstream tube and forepart of downstream tube.
c) The average Nu (Nu_m) was shown to increase by 8%-78% and it is found that the location VGs on $\Phi=120^0$ provides the best heat transfer augmentation.

REFERENCES

[1] P. Chu, Y.L. He, W.Q. Tao. 2009. Three dimensional numerical study of flow and heat transfer enhancement using vortex generators in fin and tube heat exchanger. Journal of Heat Transfer. 131. 091903-1-9.

[2] Yong Gang Lie, Ya Ling He, Li Ting Tian, Pan Chu, Wen Quan Tao. 2010. Hydrodynamics and heat transfer characteristics of a novel heat exchanger with delta winglet vortex generator, Journal of Chemical Engineering Science. 65. 1551-1562.

[3] K Thirumalai Kannan and B. Senthil Kumar. 2011. Heat Transfer and fluid flow analysis in plate fin and tube heat exchanger with different shape vortex generators, Int. Journal of Chemical Engineering Science. 357-361.

[4] Jiin Yuh Jang, Ling Fang Hsu, Jin Sheng Leu. 2013. Optimization of span angle and location of vortex generators in a plate fin and tube heat exchanger, Int. Journal of Soft Computing and Engineering. 67. 432-444.

[5] Wu, J.M., Tao, W.Q. 2007. Investigation on laminar convection heat transfer in fin-and-tube heat exchanger in aligned arrangement with longitudinal vortex generator from the viewpoint of field synergy principle, Applied Thermal Engineering 27 (14-15), 2609-2617.

[6] S.V. Patankar. Numerical Heat Transfer and Fluid Flow. Hemisphere, New York, 1980.